Non-double-couple mechanism of moderate earthquakes near Zakynthos, Greece, April 2006; explanation in terms of complexity

J. Zahradnik[1]*, E. Sokos[2], G.-A. Tselentis[2] and N. Martakis[3]

[1]*Charles University, Faculty of Mathematics and Physics, Prague, Czech Republic*, [2]*University of Patras, Seismological Laboratory, Patras, Greece* and [3]*Landtech Enterprises S.A., Athens, Greece*

ABSTRACT

Deviation of earthquakes from the double-couple mechanism is an important, but delicate tool to study their source processes. For assessing the double-couple percentage, the paper suggests to complement the standard least-square moment-tensor retrieval with a hierarchic spatio-temporal grid search, progressively closer to the true source position and time. It enables identification of the double-couple percentage convergence, while its limit is the resulting double-couple percentage value, or range. The so-called double-couple percentage (DC%) versus correlation plots are introduced and difficulties of the double-couple percentage assessment are discussed. It is proved that even close to the true source position, where the strike-dip-rake angles are already stable (within a few degrees), the double-couple percentage may still vary by dozens of per cent. Moreover, even at the optimum spatial position, the double-couple percentage estimate is extremely sensitive (0 to 100%) to small variations of the subevent origin time. This behaviour is explained in terms of the source complexity, implying a time-dependent moment tensor. Therefore, the double-couple percentage of complex events depends on the studied frequency band and, in general, also on the station azimuth. This explains broad variations of the double-couple percentage reports among seismic agencies. Three earthquakes of mutually close epicentres were investigated (Zakynthos, Western Greece, April 2006, magnitudes ~5.5) and a strong non-double-couple component of one of them was identified (double-couple percentage of about 20%). Two equivalent models of this earthquake were found: a single-event non- double-couple model, and a double-event model consisting of two double-couple sources with highly different mechanisms.

INTRODUCTION

It is believed that focal mechanisms of earthquakes not only provide information about the stress field but also about special rupture phenomena, like the crack opening, etc. That is the reason why any departure from the double-couple mechanism is interesting. Starting from the classical review papers of Julian, Miller and Foulger (1998) and Miller, Foulger and Julian (1998), the literature on this topic is growing rapidly.

Recent years have seen an increased interest in focal mechanisms of earthquakes investigated in relation with the seismic exploration. For example, it has been the case of natural events used for passive tomography (Tselentis *et al*. 2006), or the events induced during hydrofracturing (e.g. Dahm, Manthei and Eisenblaetter 1999; Nolen-Hoeksma and Ruff 2001; Rutledge, Phillips and Mayerhofer 2004). Vavrycuk (2007) investigated resolution of the borehole data.

Swarm earthquakes have been often shown to include a non-double-couple mechanism (Horalek *et al*. 2000, Horalek, Sileny and Fischer 2002; Dahm, Horalek and Sileny 2000), in particular because of their possible relation with tensile

---

*E-mail: jiri.zahradnik@mff.cuni.cz

faulting (Vavrycuk 2001, 2002). Probably the most studied are the non-double-couple components in volcanic and geothermal areas (Foulger and Julian 1993; Sarao *et al.* 2001; Foulger *et al.* 2004; Julian and Foulger 2004). Rockburst and mine-induced seismic events were also investigated in this context by, for example, Sileny and Milev (2006). For readers specifically interested in the volumetric changes, see, e.g. Campus and Faeh (1997), or Sileny and Hofstetter (2002). Vasco (1990) suggested sophisticated methods to reduce the inversion trade-off effects.

A promising innovation seems to be the study of anisotropy based on the non-double-couple mechanisms (Vavrycuk 2004). From the recent papers, see also Ardeleanu *et al.* (2005), Buforn *et al.* (2006), Cesca, Buforn and Dahm (2006). An interesting topic is the search for the connections between the non-DC events, multiple-double-couple events, segmentation of faults and their fractal properties (Frohlich, Riedesel and Apperson 1989; Yunga, Lutikov and Molchanov 2005). Critical papers emphasize difficulties in obtaining reliable non-DC components, e.g. due to noise, poor station coverage or incomplete structural models (Riedesel and Jordan 1989; Sileny 1998; Weber 2006; Hagos, Shomali and Roberts 2006). Correction for anisotropy of the medium, combined with the model probability estimate, improved the source parameter retrieval in Zollo and Bernard (1989).

Seismological centres report the complete moment tensors, thus the question of the non-double-couple reliability is also of major interest to them (Frohlich 1995; Kagan 2003; Bernardi *et al.* 2004; Braunmiller and Bernardi 2005; Pondrelli *et al.* 2006), in particular in the real-time applications (Pasyanos, Dreger and Romanowicz 1996; Rueda and Mezcua 2005; Clinton, Hauksson and Solanki 2006).

Full moment tensors, comprising both double-couple and non-double-couple components obviously provide a better fit to the data, when compared to the constrained moment tensors (deviatoric or double-couple-constrained). It is simply because the former have more free parameters. A question arises if a 'small' improvement in the fit justifies a drastic change in the physical interpretation. The f-test is used, but it faces difficulties in evaluation of the physically relevant number of the data and the degrees of freedom (Dreger and Woods 2002). The uncertainty of the parameters is computed, but problems may arise from formal evaluation of the data and structural errors (e.g. Jechumtalova and Sileny 2001). Such a critical situation lasts for years because innovative methods (including the non-double-couple mechanisms) might look more attractive than the conventional ones.

The present paper is stimulated by this alerting situation. It deals with a relatively simple case of moderate earthquakes, magnitude M∼5, large enough to provide good low-frequency signals, thus enabling deterministic waveform modelling. The aim is to show that even such a case is far from being trivial as regards retrieval of the non-double-couple mechanism. And, in this sense, the paper issues a warning against routine non-double-couple estimates and their formal use in seismic exploration.

The paper has two main parts. First, to assess the non-double-couple component, a new method is suggested, i.e., a hierarchic grid search of the centroid position and time, during which the double-couple percentage (DC%) convergence is studied. The so-called double-couple percentage versus correlation plots are introduced for that purpose. Second, combining real and synthetic data, we investigate equivalence between a double-event 100% double-couple model and a single-event non-double-couple model. Although this is mainly a methodical paper, all ideas and methods are developed for three (mutually near) M ∼ 5 earthquakes in Western Greece.

MOMENT-TENSOR RETRIEVAL AND THE ITERATIVE DECONVOLUTION

The core of the method is the so-called iterative deconvolution, originally developed for teleseismic data by Kikuchi and Kanamori (1991), often used to study complexity of earthquakes (e.g. Thio and Kanamori 1996; Tocheport *et al.* 2006). The method was modified for regional distances by Zahradnik *et al.* (2005). The modification consists in the involvement of the full Green's functions (Bouchon 1981, 2003). Possibly complex events are represented by multiple point-source models, which may represent their isolated asperities, hence the code name ISOLA. It is not a tool to reveal a complex slip distribution; it is closer to the other robust methods representing source effects with a minimum number of parameters, as in the patch method of Vallee and Bouchon (2004), whose advantage is good stability. ISOLA exists as the Fortran package and the user-friendly Fortran-Matlab tool (Sokos and Zahradnik 2008). For the previous applications of ISOLA, see http://seis30.karlov.mff.cuni.cz/. They included the following earthquakes in Greece: M6.2 Lefkada 2003, M6.7 Kythira 2006, M4.9 Amfilochia 2002 and six earthquakes of M3.4 to 4.6 in the Corinth Gulf 2001–2005.

The moment tensor is calculated by the least-square minimization of the difference between observed and synthetic data (the displacement waveforms). The parameters to be

retrieved, i.e. the moment tensor components, are represented by coefficients of a linear combination of the so-called elementary seismograms (base functions) of a given focal mechanism. The inversion is repeated for a series of trial source position and origin times, while the best position and time are grid-searched. The grid search is performed in the vicinity of the hypocentre. In this sense, an accurate hypocentre is useful, but not strictly needed. The grid search provides the best position and origin time in terms of the absolute value of the correlation coefficient between the data and synthetics (for brevity, called simply the 'correlation'), obtained automatically during the least-square inversion, without needing to calculate the time series. It is given by the scalar product between the right-hand side of the normal-equation system and the vector of the retrieved parameters. All correlation values, not just the largest one, are saved for a detailed post-evaluation of the inversion. At the best-fitting spatio-temporal position, the match between the observed and synthetic data is characterized by the overall variance reduction (over all stations and components).

It is assumed that the moment tensor is deviatoric (its volume part is vanishing). It is characterized by normalized eigenvalues 1:-f:f-1, where the minimum of their absolute values is $0 \leq f \leq 0.5$. The double-couple case is equivalent to $f = 0$, and the deviation from DC can be characterized by, for example, f or 2f. In this paper, following Knopoff and Randall (1970), we define the double-couple part of the deviatoric tensor as a tensor with the same unit eigenvectors, but with eigenvalues 1:0:-1, and refer to $100*(1–2f)$ as the double-couple percentage. If speaking about the deviatoric moment tensor orientation expressed by the strike, dip and rake, we mean just this double-couple part.

Alternatively, we perform the moment-tensor retrieval also in its double-couple-constrained mode. The (non-linear) constraint is expressed by the vanishing determinant of the moment tensor. This condition is linearized and combined with the linear least-square equation using the method of Lagrange multipliers. It yields an iterative procedure with the first approximation being represented by the double-couple part of the deviatoric solution. In each iteration step the Lagrange parameter is calculated numerically from the non-linear constraint equation. All solutions in this paper were close to the first approximation. Multiple solutions (Henry, Woodhouse and Das 2002) were not investigated.

The inversion provides a set of 'subevents', possibly representing the source complexity, whose retrieval is done by the so-called iterative deconvolution. The first subevent provides the best point-source approximation of the entire observed

waveforms, the corresponding synthetic seismograms are subtracted from the observed waveforms and the resulting residual seismograms are processed repeatedly in the same way to get the second subevent, and so on.

The input of ISOLA code is the band-passed velocity records, instrumentally corrected and later, inside ISOLA, integrated into the band-passed displacement. Complete waveforms are always used, without any need to extract a particular wave group or phase. The same filter is used for the observed and synthetic data. That is why we do not have to worry too much about the filter type (e.g., causal or non-causal). The amplitude response of the filter is characterized by four frequencies. It is flat between f2, f3, while two cosine tapers are applied at the edges between f1, f2 and f3, f4, respectively. The phase response of the filter is zero. Symbolic denotation of the frequency range, used below, is then f1;f2;f3;f4. The taper widths must be large enough to reduce ringing. Then frequency f2 is chosen as low as possible, but still having a good signal-to-noise ratio. Choice of frequency f3 is a matter of experimentation. Varying f3 may provide different physical formulations of the inversion problem; increasing f3 increases the number of subevents of comparable size, opening difficult questions about their physical reliability.

DEVIATORIC INVERSION

A sequence of more than 15 earthquakes of magnitude M > 4 occurred for a period of two months between April and May, 2006, near the Zakynthos island in Western Greece. For a comparable event of the area, see Roumelioti *et al.* (2004). More than five events had M > 4.5 and caused moderate damage. The three largest events of the series, the moment magnitude Mw $\sim$ 5.5, are the subject of the present paper. See Table 1 and Fig. 1a. The ORFEUS[1] location (Lat: 37.7°N, Lon: 20.9°E) is common to all three. The earthquakes were recorded by the broadband instruments (Nanometrics Trillium 40s) of PSLNET[2] , a new satellite telemetry network, starting operation in 2006 and belonging to the Seismological Laboratory of the University of Patras. Note that after HARVARD[3] and MEDNET[4] agencies, all three events have a similar

---

[1]ORFEUS Observatories and Research Facilities for EUropean Seismology
[2]PSLNET Patras Satellite Link NETwork
[3]HARVARD Harvard Seismology: Centroid-Moment Tensor Project
[4]MEDNET MEDiterranean Very Broadband Seismographic NETwork.

Table 1 Moment-tensor solution from several agencies

Event 1: 2006 04 11

Agency	Time (UTC)	Lat. N (deg)	Lon. E (deg)	Depth (km)	Moment (10^{18} Nm)	Mw
HARVARD	00:02:46.29	37.64	20.75	21.1	0.23	5.5
MEDNET	00:02:37.9	37.51	20.66	29.3	0.23	5.5

Agency	Strike (deg)	Dip (deg)	Rake (deg)	Strike (deg)	Dip (deg)	Rake (deg)	DC%
HARVARD	148	69	72	9	27	128	93
MEDNET	159	67	80	3	25	112	74

Event 2: 2006 04 11

Agency	Time (UTC)	Lat. N (deg)	Lon. E (deg)	Depth (km)	Moment (10^{18} Nm)	Mw
HARVARD	17:29:33.76	37.60	20.83	22.2	0.25	5.5
MEDNET	17:29:28.7	37.33	20.67	22.9	0.29	5.6
SED	17:29:27.2	37.72	20.94	18	0.37	5.7

Agency	Strike (deg)	Dip (deg)	Rake (deg)	Strike (deg)	Dip (deg)	Rake (deg)	DC%
HARVARD	167	59	71	21	36	119	24
MEDNET	164	62	70	21	33	123	30
SED	213	57	144	325	60	39	61

Event 3: 2006 04 12

Agency	Time (UTC)	Lat. N (deg)	Lon. E (deg)	Depth (km)	Moment (10^{18} Nm)	Mw
HARVARD	16:52:06.5	37.63	20.74	21.3	0.39	5.7
MEDNET	16:51:59.3	37.74	20.89	23.4	0.35	5.7

Agency	Strike (deg)	Dip (deg)	Rake (deg)	Strike (deg)	Dip (deg)	Rake (deg)	DC%
HARVARD	151	68	78	1	25	118	97
MEDNET	160	64	87	348	26	97	96

orientation of the moment tensor, a reverse mechanism, but one of them (Event 2) has a large non-DC component. Another noticeable feature of Event 2 is the larger scatter among the agency solutions.

For M5.5, according to Somerville *et al.* (1999), we expect the fault area to be of 36 km², say 6 × 6 km, with possibly two asperities and the overall duration of about 2–3 sec. Therefore, intuitively, with f < 0.1 Hz, a 'standard' M5.5 earthquake
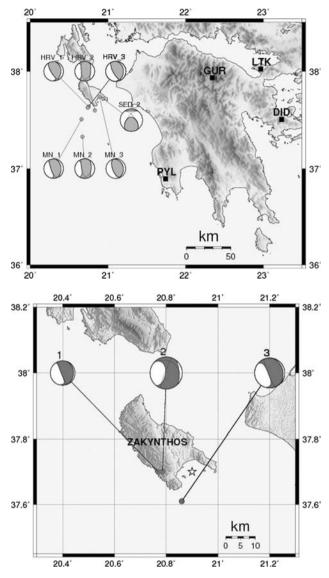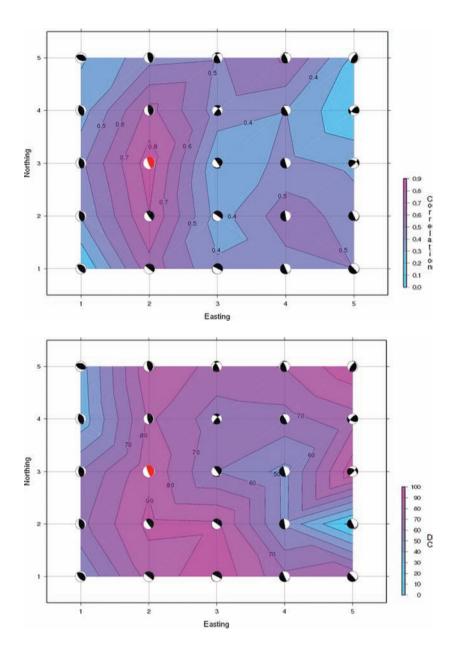
Figure 1 (a) Four broadband stations of PSLNET, a new satellite network of the University of Patras and the three earthquakes studied in this paper. The focal-mechanism solutions reported by seismological agencies are also shown (HRV = HARVARD, MN = MEDNET, and SED = Schweizerischer Erdbebendienst, Swiss Seismological Service. See also Table 1. (b) Moment tensor solutions for the three earthquakes studied in this paper. See also Table 2 Note conformity with the agency reports (Fig. 1a), in particular the large non-double-couple (DC) component of Event 2. Star denotes the ORFEUS hypocenter.

should be recognized as a single event. We do waveform inversion in the frequency ranges 0.020; 0.025; 0.08; 0.10 Hz, and discuss whether and how we 'see' the source complexity. Three mutually adjacent earthquakes will be studied under comparable conditions, and the main attention will be paid

to the different behaviour of their non-double-couple components. The spatial proximity of the events is essential; if three near events have different non-DC components, unknown details of the structural model and the limited number of stations is less critical and the differences can be more easily attributed to the source process. A 1D crustal model of Haslinger *et al.* (1999) is employed.

Event 1

The optimum source position and time are grid-searched in three stages. First we start with a 25-point grid stencil centred below the ORFEUS epicentre, with 10 km increments both in the NS direction (x, positive to N) and EW direction (y, positive to E). Based on preliminary tests, three such stencils are placed at the depths of 3, 6, and 9 km. At each depth, the moment-tensor orientation (strike, dip, rake) corresponding to the optimum time is highly variable with the trial spatial positions, except at the vicinity of the point located at x = 0, y = −10 km, i.e. 10 km west from the epicentre, where the correlation has its maximum value. As an example, Figs 2(a, b) show the situation at the depth of 6 km. To investigate the double-couple percentage we introduce the so-called double-couple percentage (DC%) versus correlation plots in Fig. 3 (bottom left). We find very large double-couple percentage changes, from 0 to 100%, even if considering only the optimum time at each space position; see the largest (red) crosses in the figure. Second, we compute the moment tensors along a vertical line passing through the optimum position from the previous stage, spanning the depths of 3, 4, . . . 10 km. Strike, dip and rake are already quite stable (154 to 160, 76 to 84, 76 to 86 degrees, respectively), with the formal, weakly pronounced optimum position at the depth of 7 km. The double-couple percentage still varies for these eight depths from 58 to 91%; Fig. 3 (bottom centre). Third, fixing the optimum depth of 7 km, we focus the spatio-temporal search to 21 trial positions between the positions (x = 0, y = −20) and (x = 0, y = −10 km). The optimum location is 11.5 km west of the epicentre. All parameters are stable in this region around the optimum position, with the strike, dip, rake = 152 to 157, 79 to 84, 81 to 82 degrees. The double-couple percentage corresponding to the optimum time has converged to a relatively narrow interval of 80 to 85%; Fig. 3 (bottom right). It is to be stressed that with an inappropriate source time (but still with a good correlation of >0.8), even just at the optimum spatial position, the double-couple percentage could be practically any value between 60 and 100%; see the chain of the medium-size (blue) crosses in Fig. 3.

Figure 2 (a) Results of the moment-tensor retrieval for Event 1 during the first (coarse) grid search of subevent 1 at a grid of 10 × 10 km increments in the West-East and South-North direction. The ORFEUS epicentre is in the middle of the plot. The optimum solution is shown in red. The background colour and contours represent the correlation between the observed and synthetic waveforms. (b) Same as in Fig. 2a, but now the background represents the double-couple percentage (DC%) value. Note that at this coarse search the focal-mechanism variations are still too large, but comparing with Fig. 2a, we already see a tendency that the largest double-couple percentage values do not follow the largest correlation, thus suggesting a need for the double-couple percentage (DC%) versus correlation study (Fig. 3).

Event 2

First, we inspect again the three depths, 3, 6, and 9 km and get the same result as for Event 1: The optimum position is at a distance of 10 km west of the ORFEUS epicentre. Second, testing a vertical line passing through this position (depth 3, 4,... 10 km) we find the best depth of 6 km. Third, using 21 trial positions on a west-east line centered at $x = 0$, $y = -10$, $z = 6$ km, we confirm the best position at that central point. Compared to Event 1, the main difference is in the double-couple percentage, see the central row of Fig. 3. Very low double-couple percentage values are detected for both the coarse search along

the vertical line (18 to 48%), as well as for the final fine search (11 to 33%). The strike-dip-rake variation for the final stage is still small, 190 to 206, 81 to 84, and 103 to 120 degrees, respectively, although larger than for Event 1.

Event 3

The same procedure as for events 1 and 2 is applied. This first search at the depths 3, 6, and 9 km points to the position $x = -10$, $y = 0$, i.e. 10 km south of the ORFEUS epicentre and the double-couple percentage is undetermined; Fig. 3 (top left). In
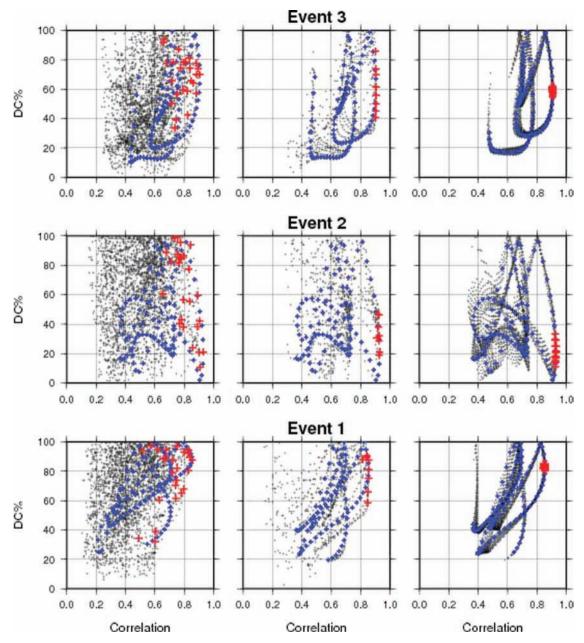
Figure 3 The double-couple percentage (DC%) versus correlation plots for the three stages of the hierarchic grid search (from the left to the right for the coarse, intermediate and fine search, respectively). Each cross corresponds to a single moment-tensor calculation of the spatio-temporal grid search. Large (red) crosses refer to the solutions at all trial spatial positions, but only at the optimum temporal position. The chain of medium-sized (blue) crosses shows the double-couple percentage variation with trial time at the optimum spatial position. Note the convergence of the double-couple percentage values (larger red symbols) when passing from the coarse to the fine search. Event 2 is anomalous as regards its low double-couple percentage, revealed under fully comparable conditions with Events 1 and 3.

the second stage, testing the latter horizontal position and the depths of 7, 8, ... 14 km, yields the depth of 11 km. Finally, with the fine search along the west-east line, we arrive at the optimum position x = −10, y = −3.5, z = 11 km. The double-couple percentage range is 40 to 85% for the vertical gridline

(Fig. 3 – top centre) and 55 to 62% for the final stage (Fig. 3 – top right). Note that the broad range of the double-couple percentage from 40 to 85% is accompanied by variations of the waveform correlation within 1%, and negligible change of the strike (155 to 158), dip (78 to 82) and rake (86 to 87)
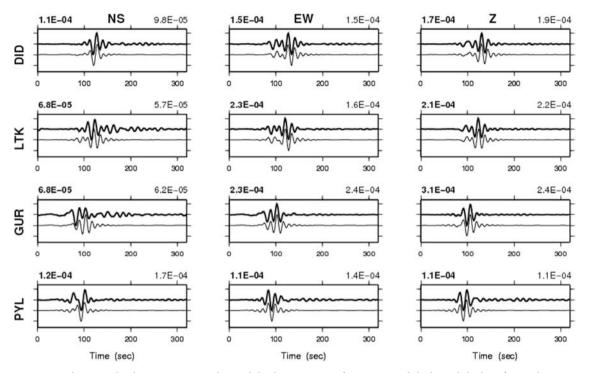
Figure 4 Comparison between the three-component observed displacement waveforms (top and thick) and the best-fitting (bottom) synthetics for Event 3. The plots are normalized to the same peak values. Their true values (in metres) are shown above the panels. The frequency range is below 0.1 Hz. For the station positions, see Fig. 1a.

Table 2 The moment-tensor solution of this paper. 'Var.red' is the overall variance reduction

Event	Date	Lat. N (deg)	Lon. E (deg)	Depth (km)	Moment (10^{18}Nm)	Strike (deg)	Dip (deg)	Rake (deg)	DC%	Var. red
1	06/04/11	37.70°	20.77°	7	0.10	157/18	80/13	82/130	83	0.73
2	06/04/11	37.70°	20.79°	6	0.19	201/306	83/26	115/16	21	0.86
3	06/04/12	37.61°	20.86°	11	0.16	158/352	80/10	87/104	58	0.82

degrees. Fig. 4 compares the observed and synthetic displacement data for the best-fitting parameters, with the overall variance reduction of 0.82.

Note that the obtained double-couple percentage range, e.g. 40 to 85% for Event 3, has no meaning of confidence interval. Investigation of the double-couple percentage error statistics is beyond the scope of this paper because we have no good measure of the data and structural model errors. Our intention was much simpler; merely to find out how large is the double-couple percentage variation compared to the "nearly constant" values of the strike, dip, and rake, near the correlation maximum. As such, the double-couple percentage range is a relative measure, useful mainly for comparing earthquakes with each other.

The optimum solutions of our study are summarized in Table 2 and Fig. 1b. The most important finding is that the double-couple percentage of the present study agrees with two agencies as regards the exceptionally large non-double-couple component of Event 2. Recall our estimate of double-couple = 21%, compared with the double-couple percentage = 24%, 30% by HARVARD and MEDNET, respectively, but all these strongly differ from the SED[5] value of 61%. Event 2 was characterized by the largest scatter among agency reports in terms of the strike, dip and rake.

[5]SED Schweizerischer Erdbebendienst, Swiss Seismological Service.

Both the low value of the double-couple percentage and large scatter of the agency reports for Event 2 are analysed in the next paragraph.

COMPARING THE DEVIATORIC AND DOUBLE-COUPLE-CONSTRAINED INVERSION

For brevity of the presentation of the double-couple-constrained inversion we do not repeat the hierarchic three-step grid search but discuss only its final fine stage (along the west-east lines of the 10 km length, sampled by 21 trial source positions). In this region we now calculate two subevents for each earthquake, and compare the deviatoric and double-couple-constrained results (Table 3 and Fig. 5).

Working very close to the correlation maximum, the correlation is a weakly varying function of the space position. Therefore, the optimum space position (and the corresponding time) may change when passing from the deviatoric to the double-couple-constrained mode. To prove a small effect of such a change on the other retrieved parameters, we tested the inversions with an additional constraint, requiring subevent

Table 3 Comparison of the deviatoric and double-couple-constrained solutions of this paper, each one with two subevents. The tensorial sum of the two double-couple subevents is also included

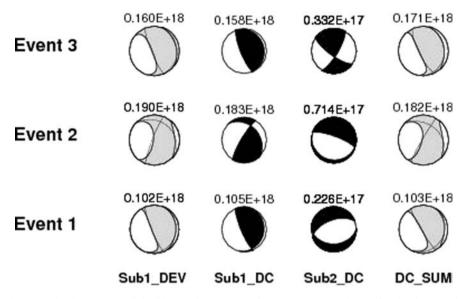| Event 1: 2006 04 11 (37.70°N, 20.77°E)								
Deviatoric solution								
Mo (Nm)	Strike	Dip	Rake	Strike	Dip	Rake	DC%	Var.red
1.03E+17	157	80	82	18	13	130	83	7.31E-01
1.79E+16	248	53	−105	93	40	−71	81	7.55E-01
Double-couple constrained solution								
1.05E+17	157	79	82	13	14	126	100	7.28E-01
2.26E+16	250	56	−101	89	36	−74	100	7.59E-01
Sum of double-couple subevent 1+subevent 2								
1.02E+17	149	82	74	33	17	154	72	7.59E-01
Event 2: 2006 04 11 (37.70°N, 20.79°E)								
Deviatoric solution								
Mo (Nm)	Strike	Dip	Rake	Strike	Dip	Rake	DC%	Var.red
1.91E+17	201	83	115	306	26	16	21	8.62E-01
4.29E+16	75	23	103	241	67	84	73	8.94E-01
Double-couple constrained solution								
1.83E+17	211	80	122	316	33	19	100	8.24E-01
7.14E+16	290	76	−88	102	14	−97	100	8.63E-01
Sum of double-couple subevent 1+subevent 2								
1.83E+17	209	86	125	305	35	7	32	8.63E-01
Event 3: 2006 04 12 (37.61°N, 20.86°E)								
Deviatoric solution								
Mo (Nm)	Strike	Dip	Rake	Strike	Dip	Rake	DC%	Var.red
1.61E+17	158	80	87	352	10	104	58	8.23E-01
2.68E+16	224	68	33	121	60	154	84	8.42E-01
Double-couple constrained solution								
1.58E+17	158	77	89	345	13	96	100	8.12E-01
3.32E+16	31	75	163	126	74	16	100	8.37E-01
Sum of double-couple subevent 1+subevent 2								
1.72E+17	154	75	82	0	17	116	73	8.37E-01

Figure 5 Comparison between the deviatoric and double-couple-constrained moment-tensor solution for the three studied earthquakes. From left to right, the 'beach balls' represent the dominant subevent of the deviatoric solution, two subevents of the double-couple-constrained solution and finally, the tensorial sum of the double-couple (DC) subevents. The sum of the two double-couple contributions is non-double-couple and equal to the deviatoric solution. Moments (in Nm) are attached to the beach balls. Event 2 has the largest non-double-couple component and two comparably strong subevents. For details, see Table 3.

1 and 2 to have the same spatial position. We found a negligible effect on the moment, strike, dip, rake and the double-couple percentage. Therefore, we present the results without this additional constraint, but do not pay any attention to the position and time. Only mentioning that with the constrained position, the temporal separation between subevents 1 and 2 in the double-couple-constrained inversion is small for all three earthquakes, 1 to 3 seconds (1 sec for Event 2).

Several important observations can be made from Table 3 and Fig. 5. (i) In general, with the double-couple-constraint, all waveform data can be matched nearly as well as in the deviatoric mode, with less than 0.03 drop in the overall variance reduction for Event 2 and even less for Events 1 and 3. (ii) Although the frequencies are low (< 0.1 Hz), subevent 2 is not negligible with respect to subevent 1. For all the three earthquakes, the moment ratio of subevent2/subevent1 does not fall below 0.17 and 0.21 in the deviatoric and DC-constrained mode, respectively. (iii) Event 2 is specific as regards its large moment ratio subevent2/subevent1 = 0.39 in the double-couple-constrained mode. (iv) Event 2 has the lowest double-couple percentage, around 20% only. (v) Subevent 1 and 2 of the double-couple-constrained inversion have strongly different focal mechanisms. (vi) Moment, as well as the strike-dip-rake angles of subevent 1 in the double-couple-constrained mode, are very close to those of subevent 1 in the deviatoric mode.

Finally, we complement the double-couple-constrained solution with the tensorial sum of the subevent 1 and 2 (also in Table 3), and compare with the deviatoric subevent 1; see again Fig. 5. Four 'beach balls' are shown for each earthquake: one for subevent 1 of the deviatoric inversion, two representing subevent 1 and 2 of the DC-constrained inversion, and one for the tensorial sum of the latter two. Very importantly, for all three earthquakes the tensorial sum of the double-couple subevents 1 and 2 is close to subevent 1 of the deviatoric mode, including the low double-couple percentage value.

To support the above observations, eight synthetic tests were also made. The aim of the tests is to understand how two 100% double-couple sources of known parameters are 'seen' by the iterative deconvolution, whether the method recognizes the complexity of the source properly, how the non-double-couple component arises due to superposition, etc. Synthetic seismograms representing the joint effect of the two 100% double-couple sources were generated for the studied stations and inverted into moment tensors in the same way as for real data. The double-couple-constrained and the deviatoric inversions were compared. The results are summarized in Fig. 6. The interest is mainly in the spatially and temporarily near sources (say a few seconds apart), analysed at relatively long periods (>10 sec), inspired by the earthquakes studied above. Tests A to H differ mainly by the moments and focal mechanisms of the studied sources. In test A there was only one
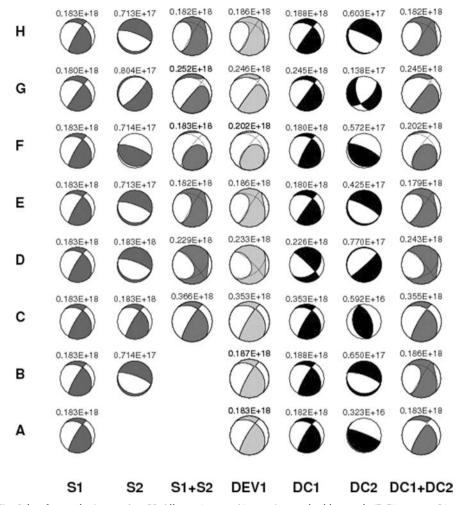
Figure 6 Similar to Fig. 5, but for synthetic tests A to H. All tests (except A) contain two double-couple (DC) sources, S1 and S2. Their separation is small so that their contributions overlap with each other (except test B, and thus S1+S2 is left empty). From left to right, the 'beach balls' represent the given 100% double-couple sources of prescribed parameters (S1 and S2), their tensorial sum (generally non-double-couple), the dominant subevent of the deviatoric inversion, two subevents obtained by the double-couple-constrained inversion, and the sum of the latter two. Note the systematic similarity between the columns 3, 4 and 7. Moments of the sources (numbers above the beach balls) are important; note that some of them are negligible, e.g. in case of the second double-couple subevent (column 6) of test A and C. Test H is analogous to test E, but with constraining subevent 2 having the same position as subevent 1.

source. Test B was specific (different from tests C to H) in studying the temporarily distant, non-overlapping sources. Test E was the one closer to Event 2 in this paper.

INTERPRETATION OF THE NON-DOUBLE-COUPLE MECHANISM

A uniform interpretation of all these experiments (real data and synthetic tests) is as follows: If two 100% double-couple sources of different focal mechanism exist in reality close to each other (temporal separation in the order of 1 sec), and their contributions overlap in the studied frequency range

(<0.1 Hz), their summary effect is equivalent to a generally non-double-couple source. In the iterative deconvolution, the first subevent tends to represent the summary effect, both in the DC-constrained and deviatoric mode. If the sum is non-double-couple, subevent 1 of the deviatoric mode will correctly reflect this fact and sufficiently describe the earthquake. On the contrary, subevent 1 of the double-couple-constrained solution will be incomplete for description of the whole event (because of its forced 100% double-couple) and therefore, a significant subevent 2 will be retrieved to compensate the missing non-double-couple part. The two models (a single non-double-couple event or a double DC event) are fully equivalent.

The last issue to be clarified is this: can the double-couple-constrained iterative deconvolution correctly identify each of the two double-couple events separately, or does it represent just their sum? The above synthetic tests are excellent tools with which to understand the situation. For example, synthetic tests C, D, G belong to the negative cases, where subevents 1 and 2 will not return the original source parameters (compare mainly the 2nd and 6th column of Fig. 6). In the trivial case of synthetic test C, where the two source contributions were identical, the double-couple-constrained inversion returns their sum in subevent 1 (while subevent 2 is negligibly small), i.e., in this case it is clearly impossible to retrieve the two events separately. The other two negative test cases (D and G) have more tricky reasons for the failure to separate event 1 and 2, related to the combination of the moment and the focal mechanism of the two events. On the other hand, synthetic tests E and F represent the positive cases, whose events 1 and 2 were successfully retrieved. As such, any double-event interpretation is to be considered with great caution and independent, additional evidence for the two events is to be sought. For example, the double-event model of the Mw6.2 Lefkada, Greece, 2003 earthquake (Zahradnik *et al.* 2005) was validated by two aftershock clusters and independently confirmed by the slip inversion (Benetatos, Dreger and Kiratzi 2007).

If we tentatively accept the double DC source model for Event 2, then the most striking feature of such an interpretation would be the large difference between the strike-dip-rake angles of the two sources. However, a closer look at Table 3 shows that in fact it does not necessarily imply a drastic change of the rupture style during the two possible source episodes, 1 and 2. Indeed, if the true fault plane was the nearly horizontal nodal plane for both, with (strike, dip, rake) = (316, 33, 19) and (102, 14, -97), respectively, then the difference is simply a 90-degree rotation between the two slip vectors, connected with just a small change of the dip during the two sub-horizontal motions. However, these speculations go beyond the scope of this paper and should not detract from the above well-justified results. Additional proof that both double-couple subevents are real would require analysis of high-frequency data.

POSSIBLE DOUBLE-COUPLE PERCENTAGE VARIATION WITH STATION SETS AND FREQUENCY

A key point of the application part of this paper was a small number and limited azimuthal coverage of the seismic stations used. In fact, we initially started with 14 stations of various networks and instruments, available through the Internet. Large problems were encountered when trying to model the waveforms from 100 to 500 km distance at frequencies below 0.1 Hz. They included long-period disturbances over small distances (Zahradnik and Plesinger 2005), problems with low S/N ratio at large distances, problems with incorrect orientation of horizontal sensors at some stations, problems with GPS synchronization of internal clocks, etc. Therefore, we decided to work with our own homogeneous network, although at that time it comprised only 4 stations (the present status, used for routine reporting of the moment tensors by the University of Patras to EMSC[6] is 7 satellite-telemetry stations). We believe that the small number of stations is not critical, since the goal was to investigate the three mutually adjacent events, hence the interest was in the relative comparison of their non-double-couple components.

Nevertheless, to validate the previous results in terms of the station configuration, we add the following synthetic test. We built up a source model comprising two 100% double-couple events of different moments (0.18e18 and 0.71e17 Nm) and different strike-dip-rake angles (211, 80, 122 and 290, 76, −88), as in Table 3 (Event 2). Both events were assumed to be in the same spatial position, mutually shifted in time by 2.8 sec. We considered 8 stations along a circle of radius 100 km, with the two sources close to its centre. The stations had an equal azimuthal separation of 45 degrees. We solved the forward problem and inverted synthetic waveforms in the deviatoric mode, with 21 trial source positions around the true one, as in the third (final) grid search in the real data case. Various station sets were used, for example, stations 2, 3, 4 (azimuths 45, 90, 135), stations 6, 7, 8 (azimuth 225, 270, 315), and all 8 stations. The strike-dip-rake angles of the two subevents were returned with a less than 10-degree error, independently of the employed station set. The double-couple percentage of subevent 1 was also stable, equal to 69%, 72% and 76% for the three sets, respectively (Fig. 7). Most importantly, Fig. 7 demonstrates that strong sensitivity of the double-couple percentage with respect to the source timing, found in real data, also persisted here for the idealized 8-station synthetic case, as marked by the chain of medium-sized (blue) crosses in Fig. 7: see the large double-couple percentage variation from 20 to 100% for the correlation >0.8.

This proves that if a double-event source is characterized by some inter-event time delay (2.8 sec) and we work at periods not very much larger (>10 seconds in our case), the

---

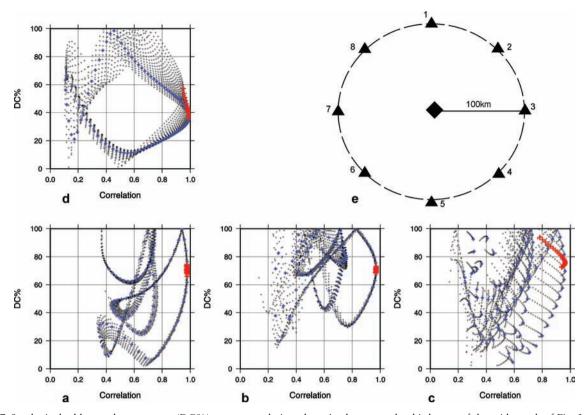[6]EMSC European-Mediterranean Seismological Centre

Figure 7 Synthetic double-couple percentage (DC%) versus correlation plots. Analogous to the third stage of the grid search of Fig. 3, but for a synthetic double DC event source. Panels *a, b, c* correspond to different station sets (stations 2,3,4; stations 6,7,8; and all 8 stations) inverted for frequency < 0.1 Hz. Panel *d* is also for all 8 stations but for < 0.04 Hz. Panel *e* explains the station configuration.

major subevent tends to approximate the temporally varying moment-tensor sum. The temporal variation of the tensor is most dramatic in its double-couple percentage; thus the resulting double-couple percentage depends strongly on the adopted approximation of the subevent origin time. The large variations of the double-couple percentage of a complex event cannot be reduced by a 'better' station configuration.

Nevertheless, there is a way to reduce the double-couple percentage variations. For the temporally varying moment tensor, the larger the studied period, the weaker the sensitivity of the double-couple percentage should be. A synthetic test enables us to make such a study for long periods, not available in the real case due to noise, say 25 to 100 seconds. The last panel (d) of Fig. 7 shows that at such a band, the chain of the medium-sized (blue) crosses at the correlation level >0.8 has reduced its double-couple percentage variation to the range of only 20 to 60%. At the same time, the formally optimum value double-couple percentage = 38% comes closer to the sum of the temporally independent tensors (32%). In this sense, the double-couple percentage of the complex events is also dependent on the studied frequency.

Much more complex would be the situation for a double-event source whose subevents have an inter-event spatial separation, 'seen' by the studied frequencies. Similarly to the apparent source time functions, the double-couple percentage then obtains an azimuthal dependence and consequently, it also depends on the station subset. (This might explain the large double-couple percentage variations with varying station sets, reported by Dreger and Woods (2002)).

We conclude this section with a new understanding of the double-couple percentage which, for complex events, is a quantity dependent on the used frequency range, and (in general) also dependent on the station azimuth. When studying three mutually adjacent events at the same stations, as in this paper, the issue is not critical but we cannot expect that other networks will generally provide the same double-couple percentage. This was nicely demonstrated by the fact that our double-couple percentage for Event 2 (close to the centroid solutions of HARVARD and MEDNET) was significantly different from SED. Note also that SED does not seek the centroid position.

CONCLUSION

To improve the waveform inversion in terms of the non-double-couple components, we introduced a new tool, the so-called double-couple percentage (DC%) versus correlation plots, calculated for a hierarchic spatio-temporal grid search. Getting progressively closer to the likely source position we identify convergence of the double-couple percentage. No formal statistics are applied to calculate the double-couple percentage confidence intervals; on the contrary, we are opponents of such a formal approach, since no appropriate estimates of the data errors are available. Our intention is much simpler; merely to find out how large is the double-couple percentage variation compared to the "nearly constant" values of the strike, dip, and rake, near the correlation maximum.

The double-couple percentage (DC%) versus correlation plots show that the variation of the double-couple percentage by dozens of per cent might be related to a correlation change of less than 1%. Such a small correlation change may correspond to a very small variation in the source position (a few kilometres) and the strike-dip-rake angles (a few degrees). As a particularly cautionary feature we demonstrate that even at the optimum space position of the source (at the formal maximum of the correlation), the double-couple percentage can still be practically any value from 0 to 100%, unless the optimum temporal position of the source is carefully examined.

The physics behind difficulties in retrieving the double-couple percentage is very simple: large double-couple percentage variations are typical for complex events. Superposition of two different double-couple sources, mutually shifted in time, is a non-double-couple moment tensor, changing with time. The orientation of the tensor (its strike-dip-rake angles) changes slowly, but the double-couple percentage changes very rapidly. As such, the resulting double-couple percentage of an earthquake depends strongly on the adopted approximation of the subevent origin time. Consequently, the double-couple percentage is also dependent on the frequency range of the inversion. Higher frequencies, sensitive to the inter-event spatial separation, may even yield an azimuthal variation of the double-couple percentage, thus also dependence on the used station subset (similarly to apparent source time functions). At very low frequencies the double-couple percentage variation is less critical, reflecting the temporally independent tensor sum. All these factors contribute to the heterogeneity of the double-couple percentage reports from seismological agencies.

Three earthquakes of M~5.5 near Zakynthos island, Western Greece (April 2006) were analysed, and one of them was identified as having a relatively strong non-double-couple component. The deviatoric inversion at periods > 10 seconds was dominated by a single subevent of the double-couple percentage of around 20% only. Using the double-couple-constrained inversion (and synthetic tests), this large departure from double-couple mechanism was interpreted in terms of two 100% double-couple events, with different focal mechanisms and a temporal separation of about 1 second. The moment ratio subevent2/subevent1 of the double DC event model was relatively large, almost 0.4, reflecting the low double-couple percentage of the non-double-couple model. The two models (a single-event non-double-couple, or a double DC event) are formally fully equivalent. Nevertheless, the complexity of this event is further supported by the heavily scattered agency estimates of the double-couple percentage, from 24 to 61%.

Finally, a remark about the usefulness of the constrained moment tensor inversion. The aim of this paper was not to imply that the deviatoric or double-couple-constrained inversion is always preferable to the full moment tensor inversion. For example, if an earthquake is a single, strongly non-double-couple event, its double-couple-constrained analysis is not appropriate. Full moment tensor analysis is good for single-event earthquakes: if the non-double-couple component of a single-event earthquake is small, then the correct full moment tensor should reflect this. On the other hand, if an earthquake is a complex event, composed of two almost purely double-couple events, the single-event interpretation with full moment tensor can provide a misleading double-couple percentage. In this sense, the main advantage of the double-couple-constrained inversion is that it can provide an independent interpretation.

REFERENCES

Ardeleanu L., Radulian M., Sileny J. and Panza G.F. 2005. Source parameters of weak crustal earthquakes of the Vrancea region from short-period waveform inversion. *Pure and Applied Geophysics* **162**, 495–513.

Benetatos C., Dreger D. and Kiratzi A. 2007. Complex and segmented rupture associated with the 14 August 2003Mw 6.2 Lefkada, Ionian Islands, earthquake. *Bulletin of the Seismological Society of America* **97**, 35–51.

Bernardi F., Braunmiller J., Kradolfer U. and Giardini D. 2004. Automatic regional moment tensor inversion in the European-Mediterranean region. *Geophysical Journal International* **157**, 703–716.

Bouchon M. 1981. A simple method to calculate Green's functions for elastic layered media. *Bulletin of the Seismological Society of America* **71**, 959–971.

Bouchon M. 2003. A review of the discrete wavenumber method. *Pure and Applied Geophysics* **160**, 445–465.

Braunmiller J. and Bernardi F. 2005. The 2003 Boumerdes, Algeria earthquake: Regional moment tensor analysis. *Geophysical Research Letters* **32**, L06305.

Buforn E., Cesca S., Goded T., del Fresno C. and Munoz D. 2006. The Bullas (Murcia, SE Spain) earthquake, 29 January 2005. *Journal of Seismology* **10**, 65–72.

Campus P. and Faeh D. 1997. Seismic monitoring of explosions: A method to extract information on the isotropic component of the seismic source. *Journal of Seismology* **1**, 205–218.

Cesca S., Buforn E. and Dahm T. 2006. Amplitude spectra moment tensor inversion of shallow earthquakes in Spain. *Geophysical Journal International* **166**, 839–854.

Clinton J.F., Hauksson E. and Solanki K. 2006. An evaluation of the SCSN moment tensor solutions: Robustness of the Mw magnitude scale, style and automation of the method. *Bulletin of the Seismological Society of America* **96**, 1689–1705.

Dahm T., Horalek J. and Sileny J. 2000. Comparison of absolute and relative moment tensor solutions for the January 1997West Bohemia earthquake swarm. *Studia Geophysica et Geodaetica* **44**, 233–250.

Dahm T., Manthei G. and Eisenblaetter J. 1999. Automated moment tensor inversion to estimate source mechanisms of hydraulically induced micro-seismicity in salt rock. *Tectonophysics* **306**, 1–17

Dreger D. and Woods B. 2002. Regional distance seismic moment tensors of nuclear explosions. *Tectonophysics* **356**, 139–156.

Foulger G.R. and Julian B.R. 1993. Non-double-couple earthquakes at the Hengill-Grensdalur volcanic complex, Iceland: Are they artefacts of crustal heterogeneity? *Bulletin of the Seismological Society of America* **83**, 38–52.

Foulger G.R., Julian B.R., Hill D.P., Pitt A.M., Malin P.E. and Shalev E. 2004. Non-double-couple microearthquakes at Long Valley caldera, California, provide evidence for hydraulic fracturing. *Journal of Volcanology and Geothermal Research* **132**, 45–71.

Frohlich C., Riedesel M.A. and Apperson K.D. 1989. Note concerning possible mechanisms for non-double-couple earthquake sources. *Geophysical Research Letters* **16**, 523–526.

Frohlich C. 1995. Characteristics of well-determined non-double-couple earthquakes in the Harvard CMT catalog. *Physics of the Earth and Planetary Interiors* **91**, 213–228.

Hagos L., Shomali H. and Roberts R. 2006. Re-evaluation of focal depths and source mechanisms of selected earthquakes in the Afar depression. *Geophysical Journal International* **167**, 297–308.

Haslinger F., Kissling E., Ansorge J., Hatzfeld D., Papadmitriou E.,

Karakostas V., Makropoulos K., Kahle H.-G. and Peter Y. 1999. 3D crustal structure from local earthquake tomography around the Gulf of Arta (Ionian region, NW Greece). *Tectonophysics* **304**, 201–218.

Henry C., Woodhouse J.H. and Das S. 2002. Stability of earthquake moment tensor inversions: Effect of the double-couple constraint. *Tectonophysics* **356**, 115–124.

Horalek J., Sileny J., Fischer T., Slancova A. and Bouskova A. 2000. Scenario of the January 1997West Bohemia Earthquake Swarm. *Studia Geophysica et Geodaetica* **44**, 491–521.

Horalek J., Sileny J. and Fischer T. 2002. Moment tensors of the January 1997earthquake swarm in NW Bohemia (Czech Republic): Double-couple vs. non-double-couple events. *Tectonophysics* **356**, 65–85.

Jechumtalova Z. and Sileny J. 2001. Point-source parameters from noisy waveforms: Error estimate by Monte-Carlo simulation. *Pure and Applied Geophysics* **158**, 1639–1654.

Julian B.R., Miller A.D. and Foulger G.R. 1998. Non-double-couple earthquake 1. Theory. *Reviews of Geophysics* **36**, 525–549.

Julian B.R. and Foulger G.R. 2004. Microearthquake focal mechanisms – A tool for monitoring geothermal systems. *Geothermal Resources Council Bulletin* **33**, 166–171.

Kagan Y.Y. 2003. Accuracy of modern global earthquake catalogs. *Physics of the Earth and Planetary Interiors* **135**, 173–209.

Kikuchi M. and Kanamori H. 1991. Inversion of complex body waves – III. *Bulletin of the Seismological Society of America* **81**, 2335–2350.

Knopoff L. and Randall M.I. 1970. The compensated linear vector dipole: A possible mechanism for deep earthquakes. *Journal of Geophysical Research* **75**, 4957–4963.

Miller A.D., Foulger G.R. and Julian B.R. 1998. Non-double-couple earthquake 2. Observations. *Reviews of Geophysics* **36**, 551–568.

Nolen-Hoeksma R.C. and Ruff L.J. 2001. Moment tensor of microseisms from the B-sand propped hydrofracture, M-site, Colorado. *Tectonophysics* **336**, 163–181.

Pasyanos M.E., Dreger D.S. and Romanowicz B. 1996. Toward real-time estimation of regional moment tensors. *Bulletin of the Seismological Society of America* **86**, 1255–1269.

Pondrelli S., Salimbeni S., Ekström G., Morelli A., Gasperini P. and Vannucci G. 2006. The Italian CMT dataset from 1977 to the present. *Physics of the Earth and Planetary Interiors* **159**, 286–303.

Roumelioti Z., Benetatos Ch., Kiratzi A., Stavrakakis G. and Melis N. 2004. A study of the 2 December 2002(M5.5) Vartholomio (western Peloponnese, Greece) earthquake and of its largest aftershocks. *Tectonophysics* **387**, 65–79.

Riedesel M.A. and Jordan T.H. 1989. Display and assessment of seismic moment tensors. *Bulletin of the Seismological Society of America* **79**, 85–100.

Rueda J. and Mezcua J. 2005. Near-real-time seismic moment-tensor determination in Spain. *Seismological Research Letters* **76**, 455–465.

Rutledge J.T., Phillips W.S. and Mayerhofer M.J. 2004. Faulting induced by forced fluid injection and fluid flow forced by faulting: An interpretation of hydraulic-fracture microseismicity, Carthage Cotton Valley Gas Field, Texas. *Bulletin of the Seismological Society of America* **94**, 1817–1830.

Sarao A., Panza G.F., Privitera E. and Cocina O. 2001. Non-double-couple mechanisms in the seismicity preceding the 1991–1993 Etna volcano eruption. *Geophysical Journal International* **145**, 319–335.

Sileny J. 1998. Earthquake source parameters and their confidence regions by a genetic algorithm with a 'memory'. *Geophysical Journal International* **134**, 228–242.

Sileny J. and Hofstetter R. 2002. Moment tensor of the 1999 Dead Sea calibration shot: Limitations in the isotropic source retrieval without a detailed earth model. *Tectonophysics* **356**, 157–169.

Sileny J. and Milev A. 2006. Seismic moment tensor resolution on a local scale: Simulated rockburst and mine-induced seismic events in the Kopanang gold mine, South Africa. *Pure and Applied Geophysics* **163**, 1495–1513.

Sokos E. and Zahradnik J. 2008. ISOLA – A Fortran code and a Matlab GUI to perform multiple-point source inversion of seismic data. *Computers and Geosciences*, in press.

Somerville P., Irikura K., Graves R., Sawada S., Wald D., Abrahamson N., Iwasaki Y., Kagawa T., Smith N. and Kowada A. 1999. Characterizing crustal earthquake slip models for the prediction of strong ground motion. *Seismological Research Letters* **70**, 59–80.

Tocheport A., Rivera L. and Van Der Woerd J. 2006. A study of the November 2001 Kokoxili Earthquake: History and geometry of the rupture from teleseismic data and field observations. *Bulletin of the Seismological Society of America* **96**, 1729–1740.

Thio H.K. and Kanamori H. 1996. Source complexity of the 1994 Northridge earthquake and its relation to aftershock mechanisms. *Bulletin of the Seismological Society of America* **86**, S84–S92.

Tselentis G.-A., Sokos E., Martakis N. and Serpetsidaki A. 2006. Seismicity and seismotectonics in Epirus, Western Greece: Results from a microearthquake survey. *Bulletin of the Seismological Society of America* **96**, 1706–1717.

Vallee M. and Bouchon M. 2004. Imaging coseismic rupture in far field by slip patches. *Geophysical Journal International* **156**, 615–630.

Vasco D.W. 1990. Moment-tensor invariants: Searching for non-double couple earthquakes. *Bulletin of the Seismological Society of America* **80**, 354–371.

Vavrycuk V. 2001. Inversion for parameters of tensile earthquakes. *Journal of Geophysical Research* **106**, 16.339–16.355.

Vavrycuk V. 2002. Non-double-couple earthquakes of 1997 January in West Bohemia, Czech Republic: Evidence of tensile faulting. *Geophysical Journal International* **149**, 365–374.

Vavrycuk V. 2004. Inversion for anisotropy from non-double-couple components of moment tensors. *Journal of Geophysical Research* **109**, B07306.

Vavrycuk V. 2007. On the retrieval of moment tensors from borehole data. *Geophysical Prospecting* **55**, 381–391.

Weber Z. 2006. Probabilistic local waveform inversion for moment tensor and hypocentral location. *Geophysical Journal International* **165**, 607–621.

Yunga S., Lutikov A. and Molchanov O. 2005. Non-double-couple seismic sources, faults interaction and hypothesis of self-organized criticality. *Natural Hazards and Earth System Sciences* **5**, 11–15.

Zahradnik J., Serpetsidaki A., Sokos E. and Tselentis G.-A. 2005. Iterative deconvolution of regional waveforms and double-event interpretation of the 2003 Lefkada earthquake, Greece. *Bulletin of the Seismological Society of America* **95**, 159–172.

Zahradnik J. and Plesinger A. 2005. Long-period pulses in broadband records of near earthquakes. *Bulletin of the Seismological Society of America* **95**, 1928–1939.

Zollo A. and Bernard P. 1989. S-wave polarization inversion of the 15 October 1979 23:19 Imperial Valley aftershock: Evidence for anisotropy and a simple source mechanism. *Geophysical Research Letters* **16**, 1047–1050.

Internet addresses of the agencies used in this paper:

http://www.seismology.harvard.edu/projects/CMT/

http://mednet.rm.ingv.it/rcmt.php

http://www.seismo.ethz.ch/moment_tensor/

http://www.orfeus-eu.org/

http://seismo.geology.upatras.gr/isola/